



This discussion paper is/has been under review for the journal Atmospheric Measurement Techniques (AMT). Please refer to the corresponding final paper in AMT if available.

High-resolution continuous flow analysis setup for water isotopic measurement from ice cores using laser spectroscopy

B. D. Emanuelsson^{1,2}, W. T. Baisden², N. A. N. Bertler^{1,2}, E. D. Keller², and V. Gkinis³

¹Antarctic Research Centre, Victoria University of Wellington, P.O. Box 600, Wellington 6140, New Zealand

²National Isotope Centre, GNS Science, 30 Gracefield Road, Lower Hutt 5010, New Zealand

³Centre for Ice and Climate, Niels Bohr Institute, University of Copenhagen, Juliane Maries Vej 30, 2100 Copenhagen, Denmark

Received: 19 September 2014 – Accepted: 7 November 2014 – Published: 2 December 2014

Correspondence to: B. D. Emanuelsson (daniel.emmanuelsson@vuw.ac.nz)

Published by Copernicus Publications on behalf of the European Geosciences Union.

High-resolution continuous flow analysis setup for water isotopic measurement

B. D. Emanuelsson et al.

Title Page

Abstract

Introduction

Conclusions

References

Tables

Figures



Back

Close

Full Screen / Esc

Printer-friendly Version

Interactive Discussion



Abstract

Here we present an experimental setup for water stable isotopes ($\delta^{18}\text{O}$ and δD) continuous flow measurements. It is the first continuous flow laser spectroscopy system that is using Off-Axis Integrated Cavity Output Spectroscopy (OA-ICOS; analyzer manufactured by Los Gatos Research – LGR) in combination with an evaporation unit to continuously analyze sample from an ice core.

A Water Vapor Isotopic Standard Source (WVISS) calibration unit, manufactured by LGR, was modified to: (1) increase the temporal resolution by reducing the response time (2) enable measurements on several water standards, and (3) to reduce the influence from memory effects. While this setup was designed for the Continuous Flow Analysis (CFA) of ice cores, it can also continuously analyze other liquid or vapor sources.

The modified setup provides a shorter response time (~ 54 and 18 s for 2013 and 2014 setup, respectively) compared to the original WVISS unit (~ 62 s), which is an improvement in measurement resolution. Another improvement compared to the original WVISS is that the modified setup has a reduced memory effect.

Stability tests comparing the modified WVISS and WVISS setups were performed and Allan deviations (σ_{Allan}) were calculated to determine precision at different averaging times. For the 2013 modified setup the precision after integration times of 10^3 s are 0.060 and 0.070 ‰ for $\delta^{18}\text{O}$ and δD , respectively. For the WVISS setup the corresponding σ_{Allan} values are 0.030 , 0.060 and 0.043 ‰ for $\delta^{18}\text{O}$, δD and $\delta^{17}\text{O}$, respectively. For the WVISS setup the precision is 0.035 , 0.070 and 0.042 ‰ after 10^3 s for $\delta^{18}\text{O}$, δD and $\delta^{17}\text{O}$, respectively. Both the modified setups and WVISS setup are influenced by instrumental drift with $\delta^{18}\text{O}$ being more drift sensitive than δD . The σ_{Allan} values for $\delta^{18}\text{O}$ of 0.30 and 0.18 ‰ for the modified (2013) and WVISS setup, respectively after averaging times of 10^4 s (2.78 h).

The Isotopic Water Analyzer (IWA)-modified WVISS setup used during the 2013 Roosevelt Island Climate Evolution (RICE) ice core processing campaign achieved

High-resolution continuous flow analysis setup for water isotopic measurement

B. D. Emanuelsson et al.

Title Page

Abstract

Introduction

Conclusions

References

Tables

Figures

◀

▶

◀

▶

Back

Close

Full Screen / Esc

Printer-friendly Version

Interactive Discussion



high precision measurements, in particular for δD , with high temporal resolution for the upper part of the core, where a seasonally resolved isotopic signal is preserved.

1 Introduction

Water stable isotopes ($\delta^{18}\text{O}$ and δD , hereafter referred to as δ) are powerful tracers for both present and past climate. The δ -notation is a common way to represent the abundance of rare isotopes as a deviation from a reference ratio: $\delta^i = \frac{R^i}{R_{\text{SMOW}}^i} - 1$, where R^i and R_{SMOW}^i are the ratio between rare and abundant isotopes $^{18}\text{O}/^{16}\text{O}$, or D/H in the sample and in VSMOW (Vienna Standard Mean Ocean Water), respectively.

Ice cores are valuable archives from which we can gain knowledge of past climate by investigating proxy records that are preserved in the ice or in entrapped gas bubbles, e.g. from water molecules, chemical impurities, particulates and methane gas (e.g. Petit et al., 1999; EPICA Community Members, 2004; WAIS Divide Project Members, 2013).

Proxy records provide important insights into Antarctic and Greenland's climate as observational data are limited to the most recent decades. Antarctic data are available from 1957 but with a bias towards coastal stations. Reliable satellite data providing extensive spatial coverage are available from 1979. Ice core proxy information offers a unique opportunity to extend the limited instrumental records (e.g. Steig et al., 2013; Thomas et al., 2013).

$\delta^{18}\text{O}$ and δD have traditionally been used as a site temperature proxy in ice core records (Epstein and Mayeda, 1953; Dansgaard, 1964), but sea ice extent, atmospheric circulation, transportation pathways, changes in source region, as well as post-depositional effects (wind scour, diffusion, etc.) influence the δ -signal (Jouzel et al., 1997; Masson-Delmotte et al., 2008; Küttel et al., 2012; Sinclair et al., 2013). Deuterium excess (d-excess) is a second-order proxy (d-excess = $\delta D - 8 \cdot \delta^{18}\text{O}$; Craig, 1963; Dansgaard, 1964) commonly interpreted as describing relative humidity and temperature at

High-resolution continuous flow analysis setup for water isotopic measurement

B. D. Emanuelsson et al.

Title Page

Abstract

Introduction

Conclusions

References

Tables

Figures

◀

▶

◀

▶

Back

Close

Full Screen / Esc

Printer-friendly Version

Interactive Discussion



the moisture source region, as a result of the kinetic isotope effect during evaporation (Merlivat and Jouzel, 1979).

Laser spectrometry has made Continuous Flow Analysis (CFA) of δ in ice core melt streams possible (Gkinis et al., 2010; Maselli et al., 2013), replacing high resolution discrete measurements for delivering near-instrumental resolution (e.g. Rhodes et al., 2012; Sinclair et al., 2013) from ice cores. Here, we describe the design and performance of laser spectrometry δ -CFA systems used for analysis of the Roosevelt Island Climate Evolution (RICE) Antarctic ice core, retrieved from (79°21'46" S, 161°42'3" W, 560 m.a.s.l.) an ice rise (Conway et al., 1999) situated at the north-eastern edge of the Ross Ice Shelf. With the objective to identify characteristic synoptic conditions in the Ross Sea region, the isotopic record's correlation with sea ice extent, atmospheric circulation modes and local temperature will be investigated using reanalysis data (1979 to 2012). Establishing correlations and transfer functions between climate drivers and the ice core record for the recent past, where there are metrological data available will be important for the interpretation of the deeper part of the record.

Laser spectroscopy was first proven as a viable alternative to isotope-ratio mass spectrometry (IRMS) by Kerstel et al. (1999). The improvements within the field of commercially available laser absorption spectroscopy analyzers (Baer et al., 2002; Crosson et al., 2008; Berman et al., 2013; Steig et al., 2014) makes them suitable to analyze water vapor continuously to achieve high temporal resolution in-situ measurement series, within a range of research areas including atmospheric sciences (Johnson et al., 2011; Steen-Larsen et al., 2013), paleoclimate ice cores records (Gkinis et al., 2010; Steig et al., 2013; Maselli et al., 2013), ecology (Lee et al., 2007) and hydrology (Goebel and Lascano, 2012).

Over recent years vaporizing units that introduce vapor from standards to the absorption spectroscopy instruments have been developed to achieve reliable calibrations (Gkinis et al., 2010; Schmidt et al., 2010; Strum and Knohl, 2010; Steig et al., 2014). There are also commercially available calibration units; Water Vapor Standard Source (WVSS) manufactured by Los Gatos Research (LGR) and Standard Delivery Module

High-resolution continuous flow analysis setup for water isotopic measurement

B. D. Emanuelsson et al.

Title Page

Abstract

Introduction

Conclusions

References

Tables

Figures



Back

Close

Full Screen / Esc

Printer-friendly Version

Interactive Discussion



High-resolution continuous flow analysis setup for water isotopic measurement

B. D. Emanuelsson et al.

Title Page

Abstract

Introduction

Conclusions

References

Tables

Figures

◀

▶

◀

▶

Back

Close

Full Screen / Esc

Printer-friendly Version

Interactive Discussion



L1115-i (25 mL min^{-1}) setup, which increases the turnover rate of the cavity, which is a contributing factor to the short response time of the IWA (Aemisegger et al., 2012).

The main system we describe (custom 2013) was developed and employed for the RICE CFA melting campaign (0 to 500 m) in 2013. It consists of a commercially available IWA from LGR, and a customized furnace and evaporation chamber, which was built and fitted inside a modified WVISS calibration unit. In addition to its function as a calibration unit, the custom vaporizer setup was used as a sample introduction system, where ice core melt stream is continuously vaporized and introduced to the IWA. A similar system (2014 custom setup) incorporating improvements was assembled for the 2014 RICE CFA melting campaign (500 to 761 m), and is described briefly.

The development of the custom δ -CFA setup for ice cores was innovative, but similar setups exist at other research institutes (e.g. Gkinis et al., 2010). However, existing δ -CFA systems for ice core analysis chose Picarro instruments. To our knowledge, we are the first research group to have developed a δ -CFA setup for ice cores using Off-Axis Integrated Cavity Output Spectroscopy (OA-ICOS; Baer et al., 2002).

We perform a detailed characterization of the custom vaporizer setup and compare the performance of the custom and WVISS vaporizers. The stability and optimal calibration frequency for the setups were investigated by calculating the Allan deviation precision (Sect. 3.1). A definition of response times is introduced and response times were calculated for the custom and WVISS setup (Sect. 3.2). The response times were compared to a similar δ -CFA ice core setup (Gkinis, 2014). The calibration method for the δ -CFA data is presented in (Sect. 3.3) and the long-term stability of the IWA-custom vaporizer setup was evaluated using measurements on a control standard over a 35 day period (Sect. 3.4). Finally, the quality of the high resolution δ -data from the RICE ice core are evaluated, by comparing the δ -measurements with discrete samples (Sect. 3.5). The overall objective of this study was to establish an experimental CFA setup for ice cores that achieves δ -measurements with high temporal resolution (sub-annual resolution) and describe its performance, operation and potential improvements.

2 Experimental

2.1 IWA-35EP/TIWA-45EP laser spectroscopy system

In this study, we use an absorption spectroscopy instrument based on OA-ICOS technology in combination with an evaporation unit to continuously analyze sample from an ice core or water standards during calibration. The absorption spectroscopy instrument is an Isotope Water Analyzer (IWA) manufactured by LGR.

The IWA-35EP analyzer uses a near-infrared, tunable diode laser, which scans over three nearby absorption peaks H_2^{16}O , H_2^{18}O , and HDO located near the $1.4\ \mu\text{m}$ wavelength. The instrument uses an OA-ICOS technique (Baer et al., 2002), where the laser is directed off-axis into an optical cavity. The semi-transparent cavity absorption cell has highly reflective mirrors, yielding an effective path length of several kilometers. The transmitted intensities are recorded by a photo detector. Laser spectroscopy analyzers are able to provide simultaneous measurements of $\delta^{18}\text{O}$, δD and water vapor mixing ratios.

Sturm and Knohl (2010) reported on temperature sensitivity of the IWA. Recent IWA models have an Enhanced Performance (EP) feature, which improved the thermal control of the cavity by keeping the temperature of the cavity ($\sim 46.3^\circ\text{C}$) stable and elevated above the ambient temperature. Recent models also have the capability to measure $\delta^{17}\text{O}$, TIWA-45EP from LGR (Berman et al., 2013) and L2140-i from Picarro (Steig et al., 2014). Our IWA-35EP analyzer was updated in December 2013 to a TIWA-45EP analyzer, which added the capability of measuring $\delta^{17}\text{O}$ using a second tunable diode laser. The update of the analyzer enabled us to include $\delta^{17}\text{O}$ in our evaluation of the WVISS and the 2014 custom setup.

2.2 Evaporation/vapor introduction systems

We evaluate the performance of two water evaporation units, the WVISS calibration unit and the custom 2013 vaporizer setup. In addition to this we present preliminary data

High-resolution continuous flow analysis setup for water isotopic measurement

B. D. Emanuelsson et al.

Title Page

Abstract

Introduction

Conclusions

References

Tables

Figures

◀

▶

◀

▶

Back

Close

Full Screen / Esc

Printer-friendly Version

Interactive Discussion



and results from the 2014 updated IWA-custom setup and new previously unpublished results from a CRDS L2140-i Picarro ice core setup (University of Copenhagen; Gkinis setup) with a custom made vaporizer (vaporizer and setup described in Gkinis et al., 2010; Steig et al., 2014).

2.2.1 WVISS system

The original WVISS unit (WVISS v.2 evaporation unit; manufactured December 2013) was setup to run a single water standard. A stream of water standard is continuously evaporated by the WVISS during calibration events. The WVISS unit consists of a heated (75 °C) 1.1 L-jar into which a nebulizer injects a constant stream of miniscule water droplets, which rapidly evaporate. For incoming dry air, the WVISS incorporates a built-in compressor and drier, but we chose to plumb to an external compressed dry air source to maximize stability and minimize noise and vibration in the laboratory. The dry air is split up into two flows inside the WVISS; one constant flow that goes through the nebulizer and the second constituting the majority of the dry air flow is regulated by a Mass Flow Controller (MFC) and is introduced to the evaporation jar. Tests of the WVISS unit were performed using external compressed dry air (< 20 ppm). When provided by the manufacturer, the nebulizer (Savillex, PFA C-flow 50 nebulizer) is set up to self-aspirate a flow of 50 $\mu\text{L min}^{-1}$ from a 0.5 L glass water bottle. We use a multi-port valve (C25-3186EMH, VICI), which enables us to use more than one water standard. Additional flow resistance introduced by the multi-port valve necessitated the use of a peristaltic pump (P2; MP², Elemental Scientific) to provide a more stable water flow to the evaporation chamber. The WVISS unit is described more in depth in Rambo et al. (2011) and Kurita et al. (2012).

The performance of a complete WVISS evaporation unit was also evaluated, using the TIWA-45EP LGR analyzer.

High-resolution continuous flow analysis setup for water isotopic measurement

B. D. Emanuelsson et al.

Title Page

Abstract

Introduction

Conclusions

References

Tables

Figures

◀

▶

◀

▶

Back

Close

Full Screen / Esc

Printer-friendly Version

Interactive Discussion



2.2.2 Experimental setup for water vapor isotope measurements

Building on the design of WVISS as a calibration unit supporting measurement of vapor samples, a key principle of our customized design was that both the ice core melt stream and isotopic standards passed through the same vaporization process.

5 All changes to the WVISS involved readily available components that could easily be integrated within the WVISS shell and controlled with the IWA-WVISS system.

In the custom setup, we modified the following aspects of the setup: (1) volume of the evaporation chamber, (2) materials, (3) evaporation temperature, (4) introduction of the sample into the carrier gas, (5) reduction of travel distances of the samples. We will
10 explain the rationale and outcome of these changes in the following section.

Volume of the evaporation chamber

We reduced the internal volume of the WVISS evaporation chamber of 1.1 L to 40 mL in the 2013 custom vaporizer. The substantially smaller volume increases the turnover rate and reduces the response time. This is particularly important when analyzing multiple standards and/or a rapidly changing continuous flow signal (e.g. from an ice
15 core). The maximum resolution will be determined by the time it takes to replace the vapor volume in the evaporation chamber.

The evaporation chamber volume is less important for one-standard calibration setups (without the requirement of rapid volume exchange) as used for example to obtain
20 real time measurements of atmospheric vapor for which the WVISS was designed (Rambo et al., 2011; Aemisegger et al., 2012).

Material

The WVISS setup has a Savilex sealed 1.1 L-jar evaporation chamber. For the 2013 setup we use borosilicate glass for the custom evaporation chamber. A cavity was
25 milled within an aluminum block to hold the glass evaporation chamber in place and

High-resolution continuous flow analysis setup for water isotopic measurement

B. D. Emanuelsson et al.

Title Page

Abstract

Introduction

Conclusions

References

Tables

Figures

◀

▶

◀

▶

Back

Close

Full Screen / Esc

Printer-friendly Version

Interactive Discussion



to the analyzer was $\sim 20\,000$ ppm. Excess vapor was vented to the atmosphere through the WVISS exhaust.

Further modifications were made in a 2014 IWA-custom setup, which uses two ceramic heating elements (122 mm, 250 W, and 230 V) to heat a stainless steel evaporation block to $165\text{ }^{\circ}\text{C}$. The block is painted with high temperature black paint, to uniformly absorb radiant heat generated by the elements within a reflective cavity. The inner surface of the block is electro-polished. The same nebulizer is used as in the 2013 setup, and the mixing chamber is of similar dimensions. Dry air is pre-warmed in baffles and introduced adjacent to the nebulizer. Compared to the 2013 setup, a higher sample flow of $\sim 150\ \mu\text{L min}^{-1}$ matched with dry air flow to achieve $\sim 20\,000$ ppm water vapor concentrations are used. Preliminary results from the 2014 setup are reported here, and differ only in the vaporizer construction, and in delivery of mixed vapor to the IWA directly through an open split, accomplished by a step in PFA tubing sizes, rather than through the WVISS plumbing system.

Reduction of travel distance of the sample

The $1/4''$ PFA tubing between the WVISS and the IWA, which provides the analyzer with sample, was kept short (59 cm) and a heat tape was wrapped around the tubing to prevent condensation and reduce adsorption to the tubing walls.

The sample flow from the ice core melthead separates the sample stream from the inner and outer parts of the core, allowing for clean chemical sampling from the inner section. For CFA δ -measurements it is not necessary to have an ultra-clean sampling regime, but we recommend taking the sample stream from the inner line, to prevent blocking of the nebulizer. The δ -measurement flow requires only 50 to $150\ \mu\text{L min}^{-1}$, and thus represents a minimal draw on the available sample volume. The melt rate was monitored to allow the association of each continuous ice core measurement with a depth.

A more detailed description of the melthead and the sealed debubbler (DB1, Fig. 2) used during the 2013 and 2014 RICE melting campaign is provided in Bigler

High-resolution continuous flow analysis setup for water isotopic measurement

B. D. Emanuelsson et al.

Title Page

Abstract

Introduction

Conclusions

References

Tables

Figures

◀

▶

◀

▶

Back

Close

Full Screen / Esc

Printer-friendly Version

Interactive Discussion



High-resolution continuous flow analysis setup for water isotopic measurement

B. D. Emanuelsson et al.

Title Page

Abstract

Introduction

Conclusions

References

Tables

Figures

◀

▶

◀

▶

Back

Close

Full Screen / Esc

Printer-friendly Version

Interactive Discussion



et al. (2011). Air bubbles were introduced after DB1 to keep the sample flow in the tubing segmented. These air bubbles were later removed in DB2 located before the multi-port valve. The multi-port valve (C25-3186EMH, VICI) enables us to switch between sample from the ice core and multiple water standards (V2, Fig. 2 and Table 1).

5 Switching between sample and calibration cycles was initiated through a control and data acquisition (DAQ) interface that was built in the LabVIEW software (National Instruments). Once the calibration cycle was initiated switches between water standards were automated. RS-232-to-usb cables were used to control and log positions of the valves (stored in calibration log files). A peristaltic pump (P2; MP², Elemental Scientific) provides a constant water flow rate of 50 to 150 $\mu\text{L min}^{-1}$ to the nebulizer (Savillex, PFA C-flow 50 nebulizer, part nr. 800-1-005-01-00). PFA tubing was used for the water and vapor flows.

15 The IWA-custom vaporizer setup has proven to be reliable. The system performed without malfunction during the entire 2013 RICE melting campaign of 35 processing days.

3 Results and discussion

3.1 Signal stability (instrument drift)

20 Stability tests were performed to determine precision for different lengths of averaging times (τ_m) and to quantify at which time scales instrumental drift affects the δ -signal (Allan, 1966; Werle, 2011). Allan deviation (σ_{Allan} , square root of Allan variance, Eq. 1; Werle, 2011) was calculated using several stability tests consisting of measurements on the (LHW) standard for extended time periods. Tests were performed on the 2013 and 2014 custom and the WVISS vaporizer at water vapor concentrations of

and 5). Analytical uncertainty in d-excess was estimated to range between 0.31 and 1.37 ‰ using Eq. (2). Peak uncertainty (1.37 ‰) occurs at the center point between calibrations (Figs. 4 and 5; 1.2 h = 4320 s) and the minimum uncertainty (0.31 ‰) occurs near calibration points, within the optimal integration time for $\delta^{18}\text{O}$ (200 s).

$$\sigma_d = \left[(\sigma_{\delta D})^2 + (8 \cdot \sigma_{\delta^{18}\text{O}})^2 \right]^{1/2} \quad (2)$$

For d-excess ice core measurements, a precision of ≤ 0.1 and ≤ 1.0 ‰ for $\delta^{18}\text{O}$ and δD , respectively, is required ($\sigma_d = 1.28$ ‰; Masson-Delmotte et al., 2008). The $\delta^{18}\text{O}$ measurements are more drift sensitive compared to δD data and are therefore the limiting factor for d-excess data. To achieve high-precision measurements for $\delta^{18}\text{O}$ (< 0.1 ‰), a standard would have to be run for drift correction every ~ 1 h which is incompatible with CFA methane gas analyses.

To reduce the response time and the influence from instrumental drift, we are currently working towards a new setup, focusing on reducing the response time and the influence from instrumental drift even further. A reduced response time would allow us to run a drift standard during melting, only missing a small quantity of ice core analysis. Such an approach would accommodate competing requirements, such as frequent calibrations for isotope measurements and long periods of uninterrupted melting for methane measurements. Furthermore, if the instrumental drift is reduced, then less frequent calibrations will be required.

3.1.2 WVSS system

For the WVSS system the optimum averaging times are 700, 1000 and 1500 s with precisions of 0.04, 0.06 and 0.04 ‰ for $\delta^{18}\text{O}$, δD and $\delta^{17}\text{O}$, respectively.

The optimal averaging time is reached faster for the custom setup compared to the WVSS system indicating that the custom setup has higher precision compared to the WVSS during shorter integration times (e.g. 0 to 300 s for $\delta^{18}\text{O}$, Fig. 4). However, the

High-resolution continuous flow analysis setup for water isotopic measurement

B. D. Emanuelsson et al.

Title Page

Abstract

Introduction

Conclusions

References

Tables

Figures

◀

▶

◀

▶

Back

Close

Full Screen / Esc

Printer-friendly Version

Interactive Discussion



IWA-custom and IWA-WVISS setups. No instrumental drift can be detected for $\delta^{18}\text{O}$ and $\delta^{17}\text{O}$ for the L2140-i setup (Figs. 4 and 6). Therefore, more frequent measurements of drift correction standards will have to be performed for the IWA-custom setups in order to achieve the high precision measurements achieved by the L2140-i setup.

3.2 Response time

Isotopic step changes between water standards are used to calculate response times for the customized and the WVISS setup (Tables 3 and 4). The water vapor concentration was kept constant over the isotopic step change ($\sim 20\,000$ ppm). Cumulative distribution functions of the log normal distribution were fitted to the isotopic steps following Gkinis et al. (2010).

$$\delta_{\text{fit}}(t) = \frac{K_1}{2} \left[1 + \operatorname{erf} \left(\frac{\ln t - t_{\text{valve}}}{S\sqrt{2}} \right) \right] + K_2 \quad (3)$$

where t is the time and K_1 , K_2 , t_{valve} and S are constants which are estimated using least square optimization (LSO). The isotopic transition period, and thus the response time, was defined between the 5 and 95 % of the total isotopic step change (Eqs. 4 and 5). Beyond these limits, it becomes difficult to distinguish a step change from random signal noise.

$$\Delta\delta_{\text{step}} = \delta_{\text{std1}} - \delta_{\text{std2}} \quad (4)$$

$$\delta_{\%} = \frac{\delta_{\text{fit}} - \delta_{\text{std2}}}{\Delta\delta_{\text{step}}} \quad (5)$$

where $\Delta\delta_{\text{step}}$ is the size of the δ -step between standard 1 (δ_{std1}) and standard 2 (δ_{std2}) and $\delta_{\%}$ is the percent change using δ -signal from the fitted function in Eq. (3) δ_{fit} .

The response times for the customized setups are ~ 54 and ~ 18 s for the 2013 and 2014 custom setup, respectively. This is an improvement compared to the WVISS setup, which has response times of ~ 62 s (Fig. 7, Tables 3 and 4).

High-resolution continuous flow analysis setup for water isotopic measurement

B. D. Emanuelsson et al.

Title Page

Abstract

Introduction

Conclusions

References

Tables

Figures

◀

▶

◀

▶

Back

Close

Full Screen / Esc

Printer-friendly Version

Interactive Discussion



High-resolution continuous flow analysis setup for water isotopic measurement

B. D. Emanuelsson et al.

Title Page

Abstract

Introduction

Conclusions

References

Tables

Figures

◀

▶

◀

▶

Back

Close

Full Screen / Esc

Printer-friendly Version

Interactive Discussion



provides the response times of the IWA. This way the evaporation chamber volume does not have to be replaced for the isotopic step to be complete. When an evaporation unit is used for switching between multiple standards and/or a changing CFA signal (e.g. from CFA sample stream from an ice core), it becomes critical to have a small evaporation chamber volume, as the vapor volume in the evaporation chamber needs to be replaced before the current signal can be analyzed.

The lag bias introduced by the IWA-vaporizer setups are negligible (for both the custom setups and WVISS setups). On average δD is lagging $\delta^{18}O$ by 1 s (Table 3). A δ -signal without lag bias enables the calculation of high-frequency d-excess values. For the WVISS and the IWA-custom 2014 setup we can also confirm there is no observable bias between $\delta^{18}O$ and $\delta^{17}O$, which is relevant for ^{17}O -excess measurements (Tables 3 and 4). Furthermore, for the custom setups we find no relationship between the size of the isotopic step and the response time, nor the response time and the direction of the step (positive or negative).

We reduced the tubing length in our system for the vapor introduction to the analyzer compared to a typical atmospheric science setup, where it is necessary to have longer air intake lines. We hypothesize that our setup experiences less adsorption to tubing walls. This is important as adsorption can cause a bias between $\delta^{18}O$ and δD . The tubing between evaporation chamber and analyzer is only 59 cm, which required orientating the analyzer with the back towards the WVISS. Moreover, we applied heat tape to the tubing to reduce adsorption to tubing walls.

3.3 Calibration

The multiple water standard calibration cycle consists of four internal standards (Fig. 8); Lower Hutt milli-q water (LHW), Working Standard 1 (WS1), RICE (derived from RICE snow) and ITASE (derived from US-ITASE, West Antarctic snow). The values of the internal standards in relation to the VSMOW/SLAP scale were determined using discrete laser absorption spectroscopy measurements on the IWA-35EP analyzer (Table 1).

deviate from our set measurement level ($\sim 20\,000$ ppm). If an offset occurred from the target water mixing ratio, the analyzer's water vapor dependence is corrected accurately if the magnitude of the offset in between calibrations is constant.

Each standard is analyzed for 500 s; the first 100 s and last 100 s of each standard measurement are discarded, to conservatively avoid influence from memory effects. Measurements shorter than 250 s are omitted. Figure 8 shows an example of the standards analyzed during a calibration cycle. Average values of 300 s were calculated for each standard.

We follow the recommendation by the International Atomic and Energy Agency (IAEA) of measuring multiple water standards for calibration (Kurita et al., 2012). We fitted a multiport valve to switch between different water standards to the nebulizer to perform calibrations. The RICE and ITASE standards are used for the two-point linear correction of the CFA-data. Correction slopes were calculated using the RICE and ITASE standards directly before and directly after each melting period. The data are normalized to the RICE standard to reduce the influence from instrument drift and WS1 is used as a control standard. The calibration and normalization were linearly time-weighted between the calibration events.

The average of correction slopes from calibrations throughout the RICE processing campaign are: $\delta^{18}\text{O} = 0.941 \pm 0.0057$ (mean $\pm 1\sigma$; $N = 324$) and $\delta\text{D} = 0.997 \pm 0.0043$. Recent studies have obtained similar correction slopes ($\delta^{18}\text{O} = 0.941 \pm 0.008$ and $\delta\text{D} = 0.994 \pm 0.003$; Aemisegger et al., 2012 and $\delta^{18}\text{O} = 0.946 \pm 0.005$ and $\delta\text{D} = 1.00 \pm 0.003$; Kurita et al., 2012) using an IWA-WVISS setup. It is important to use a two-point calibration correction, as it is not feasible to calculate correction slopes using a single standard corrections approach and any resulting deviation from the predominant slope would bias the calibration.

3.4 Long-term precision and accuracy

The RICE and ITASE standards are used for the two-point linear correction of the δ -CFA data and the RICE standard is also used for normalization to minimize in-

High-resolution continuous flow analysis setup for water isotopic measurement

B. D. Emanuelsson et al.

Title Page

Abstract

Introduction

Conclusions

References

Tables

Figures

◀

▶

◀

▶

Back

Close

Full Screen / Esc

Printer-friendly Version

Interactive Discussion



find that a linear best fit for the slopes is similar for the CFA data (8.18). The similarity of the slopes suggests that the uncorrected bias in the CFA data is negligible.

The discrete and CFA data for the 133 to 144 m section of the RICE ice core was investigated further, by creating histograms of the difference between the discrete data measured on the IWA-35EP analyzer and the CFA data. A difference was calculated for each discrete sample ($N = 215$). The CFA data averaged over the discrete vial depth intervals was calculated to make a direct comparison with the lower resolution discrete measurements.

The difference between the averaged CFA and discrete data was calculated to be $0.09 \pm 0.16\text{‰}$ and $0.70 \pm 1.07\text{‰}$ (mean $\pm 1\sigma$) for $\delta^{18}\text{O}$ and δD , respectively (Fig. 12). d-excess was calculated for the discrete and averaged CFA data, the difference being $-0.05 \pm 0.25\text{‰}$ (Fig. 12c).

4 Conclusions

This study outlines the process used to develop experimental CFA equipment for δ -measurements with high temporal resolution (sub-annual) in the RICE ice cores, and describes the performance and operation of the equipment as well as potential improvements. The continuous flow laser system is the first using OA-ICOS in combination with a vaporizer unit to continuously analyze sample from an ice core. Direct measurements of water vapor of ambient atmosphere can also be performed.

Stability tests comparing the modified WVISS and the WVISS setups were performed and Allan deviations (σ_{Allan}) were calculated to determine precision at different averaging times. For the 2013 modified setup the σ_{Allan} after integration times of 10^3 s are 0.060 and 0.070‰ for $\delta^{18}\text{O}$ and δD , respectively. For the 2014 setup the corresponding σ_{Allan} values are 0.030, 0.060 and 0.043‰ for $\delta^{18}\text{O}$, δD and $\delta^{17}\text{O}$, respectively. For the WVISS setup the precision are 0.035, 0.070 and 0.042‰ after 10^3 s for $\delta^{18}\text{O}$, δD and $\delta^{17}\text{O}$, respectively. Both the modified and WVISS setup are

High-resolution continuous flow analysis setup for water isotopic measurement

B. D. Emanuelsson et al.

Title Page

Abstract

Introduction

Conclusions

References

Tables

Figures

◀

▶

◀

▶

Back

Close

Full Screen / Esc

Printer-friendly Version

Interactive Discussion



influenced by instrumental drift and $\delta^{18}\text{O}$ is more drift sensitive than δD (Figs. 4 and 5).

The peak precision uncertainty for the 2013 custom CFA δ -data is given by the Allan deviation after 1.2 h (center point between calibrations), which is $\sim 0.17\text{‰}$ and $\sim 0.13\text{‰}$ for $\delta^{18}\text{O}$ and δD , respectively (Figs. 4 and 5). Analytical uncertainty in d-excess was estimated to range between 0.31 and 1.37‰ using Eq. (2). 1.37‰ is the peak uncertainty (Figs. 4 and 5; 1.2 h = 4320 s) and the minimum uncertainty (0.31‰) occurs near calibration points, within the optimal integration time for $\delta^{18}\text{O}$ (200 s).

Results from the University of Copenhagen setup shows that the CRDS Picarro analyzer (L2140-i) and vaporizer achieves σ_{Allan} values of 0.011‰ for $\delta^{18}\text{O}$, 0.010‰ for $\delta^{17}\text{O}$, and 0.048‰ for δD , after averaging times of 10^3 s. The University of Copenhagen setup outperforms the IWA-custom setups on the basis of precision (Figs. 4–6).

The mean response times for the customized setup are 54 and 18 s for 2013 and 2014 setup, respectively. This is an improvement compared to the WVISS setup, which has response times of 62 s. The University of Copenhagen L2140-i (Picarro) analyzer and vaporizer unit setup achieves response times of 90 s for $\delta^{18}\text{O}$ and $\delta^{17}\text{O}$, and 94 s for and δD (Fig. 8e and f, Tables 3 and 4). The IWA-custom setups (the 2014 version in particular) are more responsive compared to the IWA-WVISS and University of Copenhagen setup and can therefore provide measurements with higher temporal resolution.

The two-point calibration process was evaluated by comparing the CFA data to discrete measurements. A δD vs. $\delta^{18}\text{O}$ comparison plot (Fig. 11) revealed that that the discrete and CFA data have similar slopes: 8.18 for CFA data, and 8.21 and 8.26 for discrete data obtained from the IWA-35EP and DLT-100 measurements, respectively. This indicates that the uncorrected biased in the CFA data is negligible. The overall difference between CFA and IWA-35EP discrete measurements was $0.09 \pm 0.16\text{‰}$ and $0.70 \pm 1.07\text{‰}$ (mean $\pm 1\sigma$) for $\delta^{18}\text{O}$ and δD , respectively.

The IWA-custom vaporizer setups used during the 2013 and 2014 Roosevelt Island Climate Evolution (RICE) ice core processing campaign achieved high precision mea-

High-resolution continuous flow analysis setup for water isotopic measurement

B. D. Emanuelsson et al.

Title Page

Abstract

Introduction

Conclusions

References

Tables

Figures

◀

▶

◀

▶

Back

Close

Full Screen / Esc

Printer-friendly Version

Interactive Discussion



surements, in particular for δD , with high temporal (sub-annual) resolution for the upper part of the core.

Acknowledgements. We thank Cedric Douence, Andy Phillips for analyzing discrete samples on the DLT-100 LGR analyzer. Ed Hutchinson, Bruce Crothers, Steve Mawdesley and Rebecca Pyne for help with modification of the WVISS. Doug Baer and Manish Gupta (LGR) assisted with optimization discussions and provision of additional equipment. Stefanie Semper for LabVIEW programming.

The funding for the project was provided by the New Zealand Government through GNS Science (Global Change through Time Programme, GNS-540GCT12 and GNS-540GCT32) and Victoria University of Wellington (RDF-VUW-1103).

This work is a contribution to the Roosevelt Island Climate Evolution (RICE) Program, funded by national contributions from New Zealand, Australia, Denmark, Germany, Italy, the People's Republic of China, Sweden, United Kingdom, and the United States of America. The main logistic support was provided by Antarctica New Zealand (K049) and the US Polar Program (I-209M).

References

- Aemisegger, F., Sturm, P., Graf, P., Sodemann, H., Pfahl, S., Knohl, A., and Wernli, H.: Measuring variations of $\delta^{18}O$ and δ^2H in atmospheric water vapour using two commercial laser-based spectrometers: an instrument characterisation study, *Atmos. Meas. Tech.*, 5, 1491–1511, doi:10.5194/amt-5-1491-2012, 2012.
- Allan, D. W.: Statistics of atomic frequency standards in the near-infrared, *Proc. IEEE*, 54, 221–231, 1966.
- Baer, D. S., Paul, J. B., Gupta, M., and O'Keefe, A.: Sensitive absorption measurements in the near-infrared region using off-axis integrated cavity output spectroscopy, *Appl. Phys. B-Lasers O.*, 75, 261–265, 2002.
- Berman, E. S. F., Levin, N. E., Landais, A., Li, S., and Owano, T.: Measurement of $\delta^{18}O$, $\delta^{17}O$, and ^{17}O -excess in water by off-axis integrated cavity output spectroscopy and isotope ratio mass spectrometry, *Anal. Chem.*, 85, 10392–10398, 2013.

High-resolution continuous flow analysis setup for water isotopic measurement

B. D. Emanuelsson et al.

Title Page

Abstract

Introduction

Conclusions

References

Tables

Figures

◀

▶

◀

▶

Back

Close

Full Screen / Esc

Printer-friendly Version

Interactive Discussion



High-resolution continuous flow analysis setup for water isotopic measurement

B. D. Emanuelsson et al.

Title Page

Abstract

Introduction

Conclusions

References

Tables

Figures

◀

▶

◀

▶

Back

Close

Full Screen / Esc

Printer-friendly Version

Interactive Discussion



Bigler, M., Svensson, A., Kettner, E., Vallelonga, P., Nielsen, M. E., and Steffensen, J. P.: Optimization of high-resolution continuous flow analysis for transient climate signals in ice cores, *Environ. Sci. Technol.*, 45, 4483–4489, 2011.

Conway, H., Hall, B. L., Denton, G. H., Gades, A. M., and Waddington, E. D.: Past and future grounding-line retreat of the West Antarctic Ice Sheet, *Science*, 286, 280–283, 1999.

Craig, H., Gordon, L. I., and Horibe, Y.: Isotopic exchange effects on evaporation of water: 1 low-temperature experimental results, *J. Geophys. Res.*, 68, 5079–5087, 1963.

Crosson, E. R.: A cavity ring-down analyzer for measuring atmospheric levels of methane, carbon dioxide and water vapor, *Appl. Phys. B-Lasers O.*, 92, 403–408, 2008.

Dansgaard, W.: Stable isotopes in precipitation, *Tellus*, 16, 436–468, 1964.

EPICA Community Members: Eight glacial cycles from an Antarctic ice core, *Nature*, 429, 623–628, 2004.

Epstein, S. and Mayeda, T.: Variations of ^{18}O content of waters from natural sources, *Geochim. Cosmochim. Ac.*, 4, 213–224, 1953.

Gkinis, V., Popp, T. J., Johnsen, S. J., and Blunier, T. A.: Continuous stream flash evaporator for the calibration of an IR cavity ring-down spectrometer for the isotopic analysis of water, *Isot. Environ. Healt. S.*, 46, 463–475, 2010.

Gkinis, V., Popp, T. J., Blunier, T., Bigler, M., Schüpbach, S., Kettner, E., and Johnsen, S. J.: Water isotopic ratios from a continuously melted ice core sample, *Atmos. Meas. Tech.*, 4, 2531–2542, doi:10.5194/amt-4-2531-2011, 2011.

Goebel, T. S. and Lascano, R. J.: System for high throughput water extraction from soil material for stable isotope analysis of water, *Journal of Analytical Sciences, Methods and Instrumentation*, 2, 203–207, 2012.

Johnson, L. R., Sharp, Z. D., Galewsky, J., Strong, M., Van Pelt, A. D., Dong, F., and Noone, D.: Hydrogen isotope correction for laser instrument measurement bias at low water vapor concentration using conventional isotope analyses: application to measurements from Mauna Loa Observatory, Hawaii, *Rapid Commun. Mass Sp.*, 25, 608–616, 2011.

Jouzel, J., Alley, R. B., Cuffey, K. M., Dansgaard, W., Grootes, P., Hoffmann, G., Johnsen, S. J., Koster, R. D., Peel, D., Shuman, C. A., Stievenard, M., Stuiver, M., and White, J.: Validity of the temperature reconstruction from water isotopes in ice cores, *J. Geophys. Res.*, 102, 26471–26487, 1997.

**High-resolution
continuous flow
analysis setup for
water isotopic
measurement**

B. D. Emanuelsson et al.

Title Page

Abstract

Introduction

Conclusions

References

Tables

Figures

◀

▶

◀

▶

Back

Close

Full Screen / Esc

Printer-friendly Version

Interactive Discussion



Kerstel, E. R. T., van Trigt, R., Dam, N., Reuss, J., and Meijer, H. A. J.: Simultaneous determination of the $^2\text{H}/^1\text{H}$, $^{17}\text{O}/^{16}\text{O}$ and $^{18}\text{O}/^{16}\text{O}$ isotope abundance ratios in water by means of laser spectrometry, *Anal. Chem.*, 71, 5297–5303, 1999.

Kurita, N., Newman, B. D., Araguas-Araguas, L. J., and Aggarwal, P.: Evaluation of continuous water vapor δD and $\delta^{18}\text{O}$ measurements by off-axis integrated cavity output spectroscopy, *Atmos. Meas. Tech.*, 5, 2069–2080, doi:10.5194/amt-5-2069-2012, 2012.

Küttel, M., Steig, E. J., Ding, Q., Monaghan, A. J., and Battisti, D. S.: Seasonal climate information preserved in West Antarctic ice core water isotopes: relationships to temperature, large-scale circulation, and sea ice, *Clim. Dynam.*, 39, 1841–1857, 2012.

Lee, X., Kim, K., and Smith, R.: Temporal variations of the $^{18}\text{O}/^{16}\text{O}$ signal of the whole-canopy transpiration in a temperate forest, *Global Biogeochem. Cy.*, 21, GB3013, doi:10.1029/2006GB002871, 2007.

Maselli, O. J., Fritzsche, D., Layman, L., McConnell, J. R., and Meyer, H.: Comparison of water isotope-ratio determinations using two cavity ring-down instruments and classical mass spectrometry in continuous ice-core analysis, *Isot. Environ. Health. S.*, 49, 387–398, 2013.

Masson-Delmotte, V., Hou, S., Ekaykin, A., Jouzel, J., Aristarain, A., Bernardo, R. T., Bromwich, D., Cattani, O., Delmotte, S. M., Falourd, M., Frezzotti, H., Genoni Galle, L., Isaksen, E., Landais, A., Helsen, M. M., Hoffmann, G., Lopez, J., Morgan, V., Motoyama, H., Noone, D., Oerter, H., Petit, J. R., Royer, A., Uemura, R., Schmidt, G. A., Schlosser, E., Simes, J. C., Steig, E. J., Stenni, B., Stievenard, M., van den Broeke, M. R., van de Wal, R. S. W., van de Berg, W. J., Vimeux, F., and White, J. W. C.: A review of Antarctic surface snow isotopic composition: observations, atmospheric circulation, and isotopic modeling, *J. Climate*, 21, 3359–3387, 2008.

Merlivat, L. and Jouzel, J.: Global climatic interpretation of the deuterium-oxygen 18 relationship for precipitation, *J. Geophys. Res.*, 84, 5029–5033, 1979.

Petit, J. R., Jouzel, J., Raynaud, D., Barkov, N. I., Barnola, J.-M., Basile, I., Bender, M., Chappellaz, J., Davis, M., Delaygue, G., Delmotte, M., Kotlyakov, V. M., Legrand, M., Lipenkov, V. Y., Lorius, C., Pépin, L., Ritz, C., Saltzman, E., and Stievenard, M.: Climate and atmospheric history of the past 420,000 years from the Vostok ice core, *Antarctica, Nature*, 399, 429–436, 1999.

Rambo, J., Lai, C.-T., Farlin, J., Schroeder, M., and Bible, K.: On-site calibration for high precision measurements of water vapor isotope ratios using off-axis cavity-enhanced absorption spectroscopy, *J. Atmos. Ocean. Tech.*, 28, 1448–1457, 2011.

High-resolution continuous flow analysis setup for water isotopic measurement

B. D. Emanuelsson et al.

Title Page

Abstract

Introduction

Conclusions

References

Tables

Figures

◀

▶

◀

▶

Back

Close

Full Screen / Esc

Printer-friendly Version

Interactive Discussion



Rhodes, R. H., Bertler, N. A. N., Baker, J. A., Steen-Larsen, H. C., Sneed, S. B., Morgestern, U., and Johnsen, S. J.: Little Ice Age climate and oceanic conditions of the Ross Sea, Antarctica from a coastal ice core record, *Clim. Past*, 8, 1223–1238, doi:10.5194/cp-8-1223-2012, 2012.

5 Sinclair, K. E., Bertler, N. A. N., Trompetter, W. J., and Baisden, W. T.: Seasonality of airmass pathways to coastal Antarctica: ramifications for interpreting high-resolution ice core records, *J. Climate*, 26, 2065–2076, 2013.

10 Steen-Larsen, H. C., Johnsen, S. J., Masson-Delmotte, V., Stenni, B., Risi, C., Sodemann, H., Balslev-Clausen, D., Blunier, T., Dahl-Jensen, D., Ellehøj, M. D., Falourd, S., Grindsted, A., Gkinis, V., Jouzel, J., Popp, T., Sheldon, S., Simonsen, S. B., Sjolte, J., Steffensen, J. P., Sperlich, P., Sveinbjörnsdóttir, A. E., Vinther, B. M., and White, J. W. C.: Continuous monitoring of summer surface water vapor isotopic composition above the Greenland Ice Sheet, *Atmos. Chem. Phys.*, 13, 4815–4828, doi:10.5194/acp-13-4815-2013, 2013.

15 Steig, E. J., Ding, Q., White, J. W. C., Küttel, M., Rupper, S. B., Neumann, T. A., Neff, P. D., Gallant, A. J. E., Mayewski, P. A., Taylor, K. C., Hoffmann, G., Dixon, D. A., Schoenemann, S. W., Markle, B. R., Fudge, T. J., Schneider, D. P., Schauer, A. J., Teel, R. P., Vaughn, B. H., Burgener, L., Williams, J., and Korotkikh, E.: Recent climate and ice-sheet changes in West Antarctica compared with the past 2,000 years, *Nat. Geosci.*, 6, 372–375, 2013.

20 Steig, E. J., Gkinis, V., Schauer, A. J., Schoenemann, S. W., Samek, K., Hoffnagle, J., Dennis, K. J., and Tan, S. M.: Calibrated high-precision ^{17}O -excess measurements using cavity ring-down spectroscopy with laser-current-tuned cavity resonance, *Atmos. Meas. Tech.*, 7, 2421–2435, doi:10.5194/amt-7-2421-2014, 2014.

25 Sturm, P. and Knohl, A.: Water vapor $\delta^2\text{H}$ and $\delta^{18}\text{O}$ measurements using off-axis integrated cavity output spectroscopy, *Atmos. Meas. Tech.*, 3, 67–77, doi:10.5194/amt-3-67-2010, 2010.

Thomas, E. R., Bracegirdle, T. J., Turner, J., and Wolff, E. W.: A 308 year record of climate variability in West Antarctica, *Geophys. Res. Lett.*, 40, 5492–5496, 2013.

30 Tremoy, G., Vimeux, F., Cattani, O., Mayaki, S., Souley, I., and Favreau, G.: Measurements of water vapor isotope ratios with wavelength-scanned cavity ring-down spectroscopy technology: new insights and important caveats for deuterium excess measurements in tropical areas in comparison with isotope-ratio mass spectrometry, *Rapid Commun. Mass Sp.*, 25, 3469–3480, 2011.

WAIS Divide Project Members: Onset of deglacial warming in West Antarctica driven by local orbital forcing, *Nature*, 500, 440–444, 2013.

Werle, P.: Accuracy and precision of laser spectrometers for trace gas sensing in the presence of optical fringes and atmospheric turbulence, *Appl. Phys. B-Lasers O.*, 102, 313–329, 2011.

AMTD

7, 12081–12124, 2014

High-resolution continuous flow analysis setup for water isotopic measurement

B. D. Emanuelsson et al.

Title Page

Abstract

Introduction

Conclusions

References

Tables

Figures



Back

Close

Full Screen / Esc

Printer-friendly Version

Interactive Discussion



High-resolution continuous flow analysis setup for water isotopic measurement

B. D. Emanuelsson et al.

Table 1. $\delta^{18}\text{O}$ and δD discrete-IWA measurements of water standards in relation to the VSMOW/SLAP scale.

Standard	<i>N</i>	$\delta^{18}\text{O}$ (‰)	$\pm\sigma$	δD (‰)	$\pm\sigma$
WS 1	4	−10.84	0.099	−74.15	0.938
RICE	30	−22.54	0.049	−175.02	0.193
ITASE	30	−37.39	0.046	−299.66	0.183

Title Page

Abstract

Introduction

Conclusions

References

Tables

Figures

◀

▶

◀

▶

Back

Close

Full Screen / Esc

Printer-friendly Version

Interactive Discussion

High-resolution continuous flow analysis setup for water isotopic measurement

B. D. Emanuelsson et al.

Title Page

Abstract

Introduction

Conclusions

References

Tables

Figures

◀

▶

◀

▶

Back

Close

Full Screen / Esc

Printer-friendly Version

Interactive Discussion

Table 2. Date, duration, mean water vapor concentration and standard deviation for stability tests.

Date	Setup	Duration (h)	Mean (ppm)	Std (ppm)
24 May 2013	Custom 2013	18.45	21 466	639
1 Jun 2013	Custom 2013	23.81	19 941	479
9 Jun 2013	Custom 2013	22.04	19 530	400
23 Jun 2013	Custom 2013	23.98	19 870	456
29 Jun 2013	Custom 2013	23.26	19 642	401
24 Jan 2014	WVISS	31.22	18 092	145
28 Jan 2014	WVISS	24.47	19 770	135
30 Jan 2014	WVISS	31.67	19 641	144
19 Jul 2014	Custom 2014	30.49	20 216	304
20 Jul 2014	Custom 2014	18.92	21 486	132
30 May 2014	Gkinis (2014)	30.00	–	–

High-resolution continuous flow analysis setup for water isotopic measurement

B. D. Emanuelsson et al.

Table 3. Response times for $\delta^{18}\text{O}$ and δD from isotopic step tests between water standards.

Isotopic Step	Setup	Step	$\Delta^{18}\text{O}$ (‰)	ΔD (‰)	# steps	Response time (s)						
						$\delta^{18}\text{O}$ mean	$\pm\sigma$	fit mean rmse	δD mean	$\pm\sigma$	fit mean rmse	
ITASE	RICE	Custom 2013	Pos.	14.5	124.2	5	53.4	1.9	0.51	54.1	1.7	0.51
RICE	ITASE	Custom 2013	Neg.	14.5	124.2	10	54.6	1.8	0.54	55.6	0.9	1.56
RICE	ITASE	WVISS	Neg.	14.5	124.2	7	61.3	2.6	0.55	61.8	2.4	1.82
ITASE	RICE	WVISS	Pos.	14.5	124.2	3	61.7	3.3	0.57	63.1	3.6	0.81
RICE	ITASE	Custom 2014	Neg.	14.5	124.2	10	18.4	0.8	0.48	18.5	1.0	1.56
ITASE	WS 1	Custom 2014	Pos.	26.5	225.5	7	18.4	0.9	0.44	18.8	0.5	0.67
Standard-40	CPH-DI	Gkinis 2014	Pos.	31.6	252.6	1	90.3	–	0.33	93.6	–	1.03

Title Page

Abstract

Introduction

Conclusions

References

Tables

Figures

◀

▶

◀

▶

Back

Close

Full Screen / Esc

Printer-friendly Version

Interactive Discussion



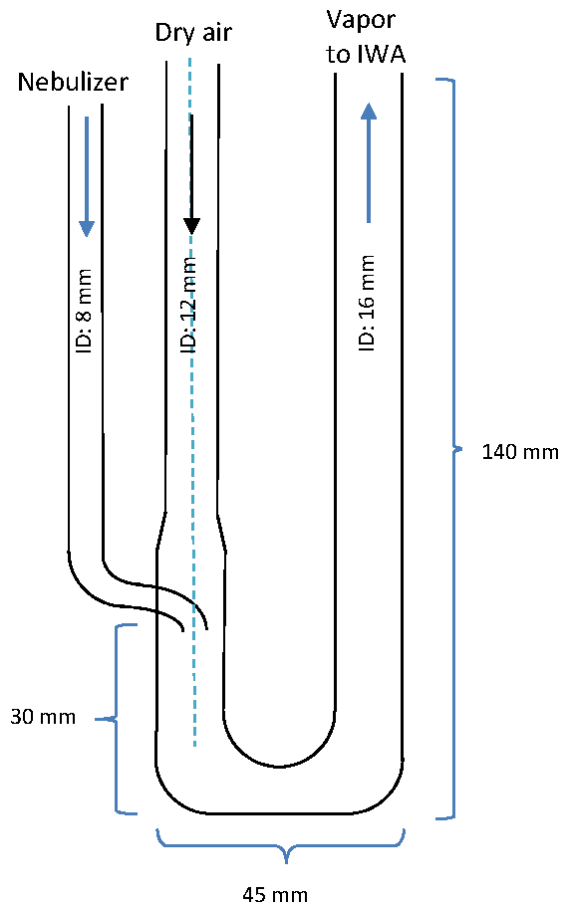


Figure 1. Drawing of glass evaporation chamber. A moist air stream is generated from the nebulizer, merged with the MFC regulated dry air, is mixed at 170°C and subsequently flows out of the glass evaporation chamber to the IWA.

12113

AMTD

7, 12081–12124, 2014

High-resolution continuous flow analysis setup for water isotopic measurement

B. D. Emanuelsson et al.

Title Page

Abstract

Introduction

Conclusions

References

Tables

Figures

◀

▶

◀

▶

Back

Close

Full Screen / Esc

Printer-friendly Version

Interactive Discussion



High-resolution continuous flow analysis setup for water isotopic measurement

B. D. Emanuelsson et al.

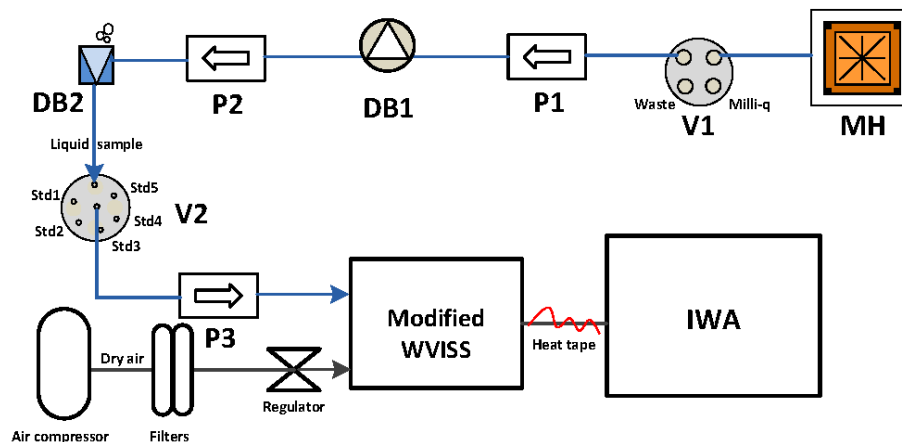


Figure 2. Flow chart of CFA IWA-custom vaporizer setup, where MH stands for melt head, V for valve, P for peristaltic pump and DB for debubbler. Blue lines represent the liquid part of the setup and the black lines represent the dry and moist air portion.

Title Page

Abstract

Introduction

Conclusions

References

Tables

Figures

◀

▶

◀

▶

Back

Close

Full Screen / Esc

Printer-friendly Version

Interactive Discussion

High-resolution continuous flow analysis setup for water isotopic measurement

B. D. Emanuelsson et al.

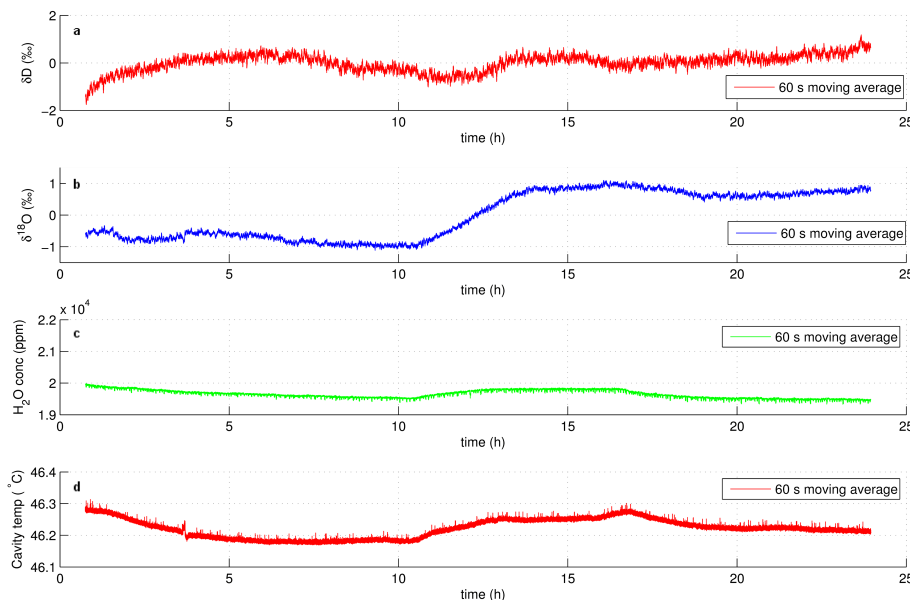


Figure 3. Shows results from a stability test using the 2013 custom vaporizer setup, measured over a 24 h period. 60 s moving averages of the 2 Hz-data is displayed. Deviation from mean value is shown for each point in **(a)** for δD and **(b)** for $\delta^{18}O$. **(c)** shows water vapor concentration (ppm), and **(d)** shows analyzer cavity temperature ($^{\circ}C$).

[Title Page](#)[Abstract](#)[Introduction](#)[Conclusions](#)[References](#)[Tables](#)[Figures](#)[◀](#)[▶](#)[◀](#)[▶](#)[Back](#)[Close](#)[Full Screen / Esc](#)[Printer-friendly Version](#)[Interactive Discussion](#)

High-resolution continuous flow analysis setup for water isotopic measurement

B. D. Emanuelsson et al.

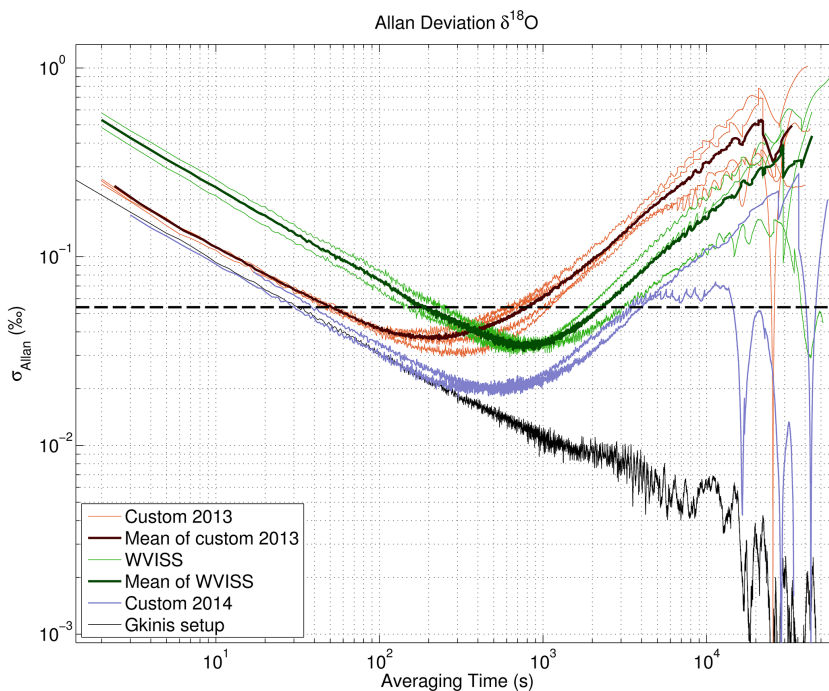


Figure 4. Allan deviation as a function of averaging time for $\delta^{18}\text{O}$ from stability tests of the custom vaporizer setups (2013 setup brown lines and 2014 setup blue lines), the WVISS setup (green line) and from the University of Copenhagen setup (Gkinis; black line). Average precision (1σ ; standard deviation) for individual discrete samples measured on the IWA-35EP analyzer is shown as a black dashed horizontal line.

[Title Page](#)[Abstract](#)[Introduction](#)[Conclusions](#)[References](#)[Tables](#)[Figures](#)[◀](#)[▶](#)[◀](#)[▶](#)[Back](#)[Close](#)[Full Screen / Esc](#)[Printer-friendly Version](#)[Interactive Discussion](#)

High-resolution continuous flow analysis setup for water isotopic measurement

B. D. Emanuelsson et al.

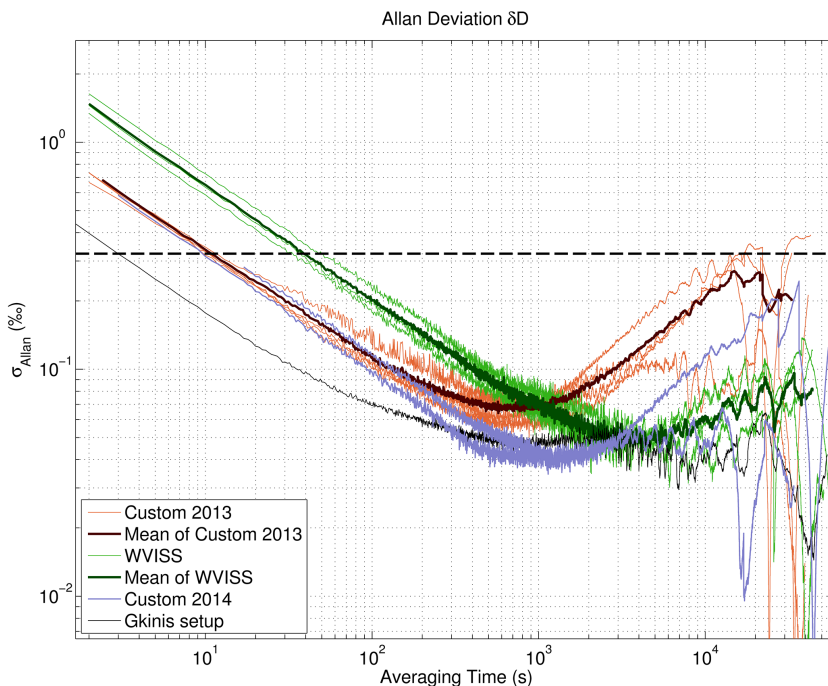


Figure 5. Allan deviation as a function of averaging time for δD from stability tests of the custom vaporizer setups (2013 setup brown lines and 2014 setup blue lines), the WVISS setup (green line) and from the University of Copenhagen setup (Gkinis; black line). Average precision (1σ ; standard deviation) for individual discrete samples measured on the IWA-35EP analyzer is shown as a black dashed horizontal line.

[Title Page](#)[Abstract](#)[Introduction](#)[Conclusions](#)[References](#)[Tables](#)[Figures](#)[◀](#)[▶](#)[◀](#)[▶](#)[Back](#)[Close](#)[Full Screen / Esc](#)[Printer-friendly Version](#)[Interactive Discussion](#)

High-resolution continuous flow analysis setup for water isotopic measurement

B. D. Emanuelsson et al.

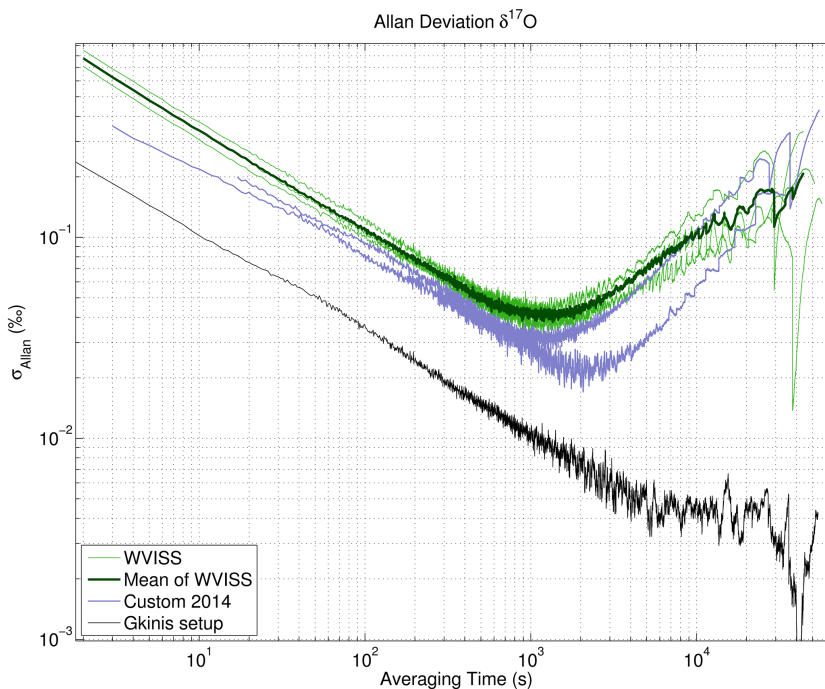


Figure 6. Allan deviation as a function of averaging time for $\delta^{17}\text{O}$ for stability tests on the WVISS setup (green lines), the 2014 custom setup (blue lines) and from the University of Copenhagen setup (Gkinis; black line).

Title Page

Abstract

Introduction

Conclusions

References

Tables

Figures

◀

▶

◀

▶

Back

Close

Full Screen / Esc

Printer-friendly Version

Interactive Discussion

High-resolution continuous flow analysis setup for water isotopic measurement

B. D. Emanuelsson et al.

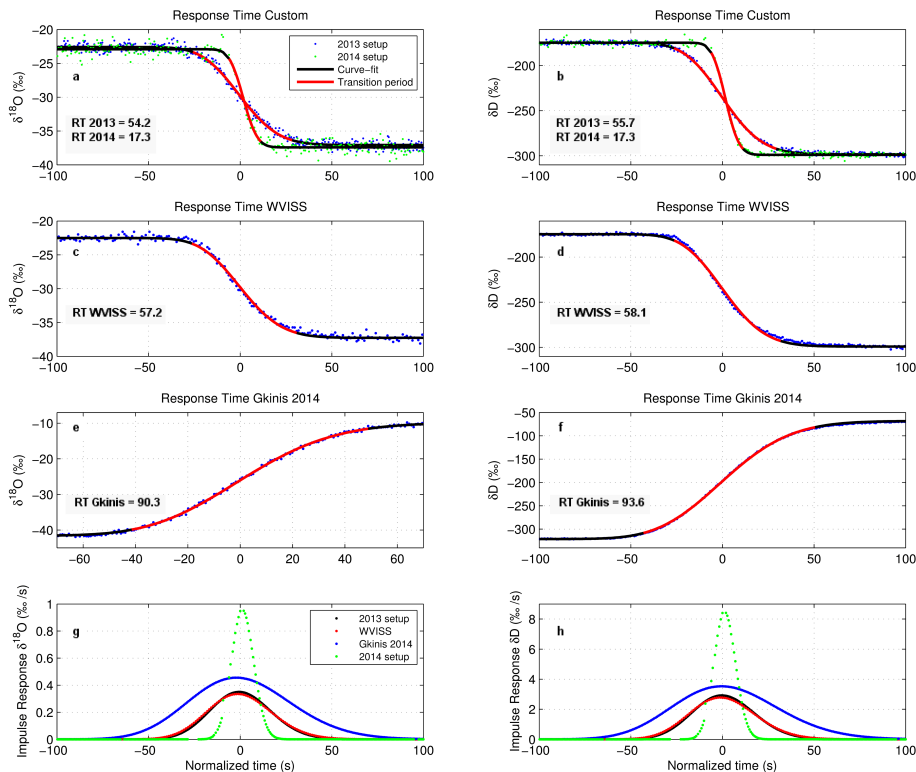


Figure 7. (a–f) shows δ -CFA data (blue dots and green dots for the 2013 and 2014 custom setup, respectively), a LSO fitted curve (black line), 5 and 95 % of change in the response time (RT) transition period (red line) for the custom setups (a and b) and WVISS setup (c and d) and the University of Copenhagen setup (Gkinis, 2014; e and f). (g, h) shows the impulse response function for the fit for the 2013 custom (black line), the 2014 custom (green line), the Gkinis (2014) (blue line), and the WVISS (red line) setup. The left column of plots (a, c, e and g) are for $\delta^{18}\text{O}$ and the right column of plots (b, d, f and h) are for δD .

High-resolution continuous flow analysis setup for water isotopic measurement

B. D. Emanuelsson et al.

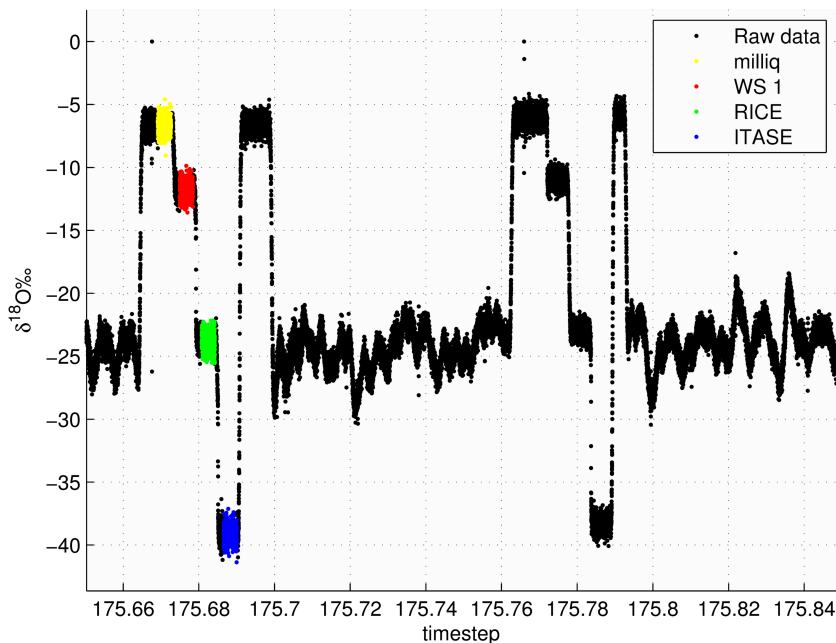


Figure 8. Example of raw-data from a melting session and calibration events from 25 June 2013. 1 m ice core sections were stacked on top each other during melting sessions. The ice core data are bracketed by calibration events. Water standards from the first calibration event are color marked. Yellow marking is for LHW standard, red for WS1, green for RICE, and blue for the ITASE water standard.

[Title Page](#)[Abstract](#)[Introduction](#)[Conclusions](#)[References](#)[Tables](#)[Figures](#)[◀](#)[▶](#)[◀](#)[▶](#)[Back](#)[Close](#)[Full Screen / Esc](#)[Printer-friendly Version](#)[Interactive Discussion](#)

High-resolution continuous flow analysis setup for water isotopic measurement

B. D. Emanuelsson et al.

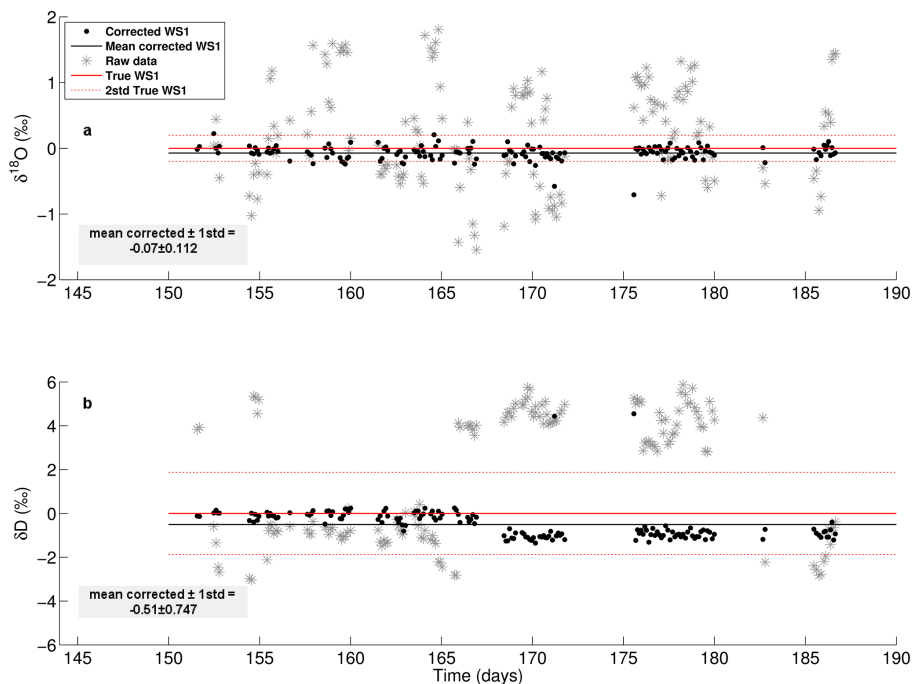


Figure 9. Normalized measurement of control standard (WS1) over 35 days. Raw data are shown as gray stars and corrected data as black dots **(a)** for $\delta^{18}\text{O}$ and **(b)** for δD . The corrected data has a standard deviation of 0.11 and 0.75 ‰ for $\delta^{18}\text{O}$ and δD , respectively. The mean corrected anomaly (black line) from the true WS1 standard value (thick red line) is -0.07 and -0.51 ‰ for $\delta^{18}\text{O}$ and δD , respectively.

High-resolution continuous flow analysis setup for water isotopic measurement

B. D. Emanuelsson et al.

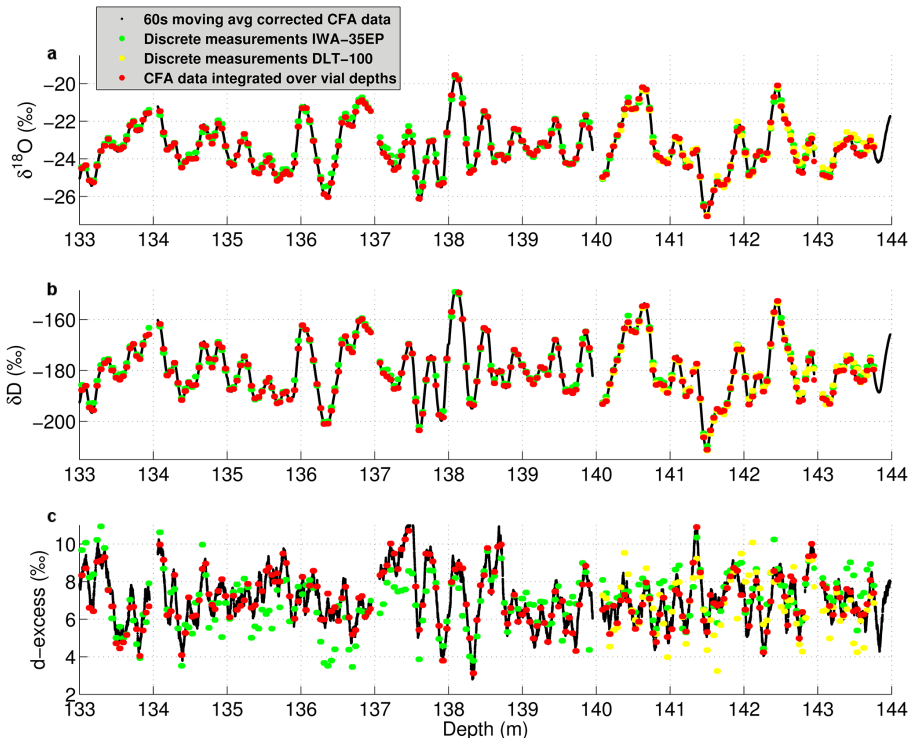


Figure 10. Shows the 60 s moving average of the corrected 2hz δ -CFA data (black line), results from discrete measurements (green dots for measurements from the IWA-35EP analyzer and yellow dots for measurements on the DLT-100 analyzer), and δ -CFA data integrated over the discrete vial depth intervals (red dots); **(a)** for $\delta^{18}\text{O}$, **(b)** for δD , and **(c)** for d-excess.

High-resolution continuous flow analysis setup for water isotopic measurement

B. D. Emanuelsson et al.

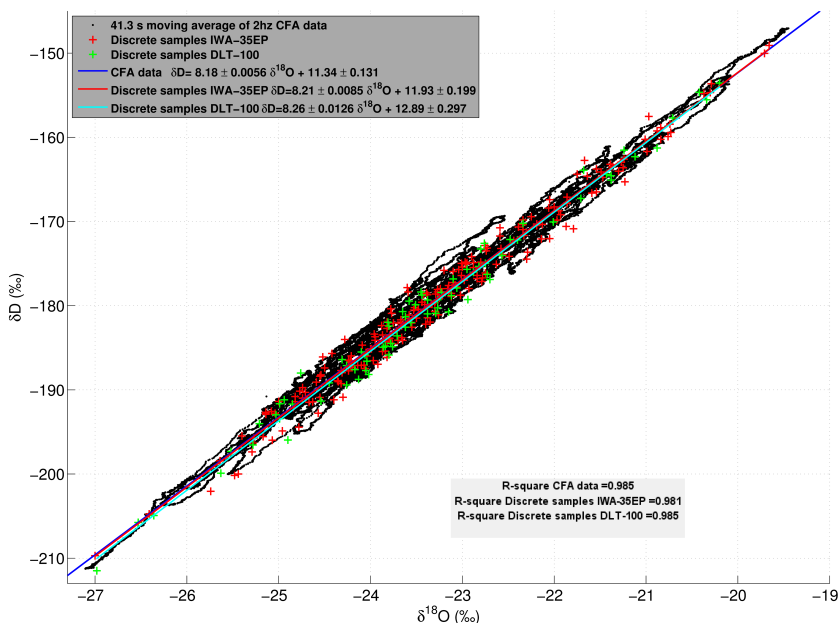


Figure 11. δD vs. $\delta^{18}\text{O}$ for 41.3 s moving average of the CFA data (black dots), discrete data measured on a DLT-100 analyzer (green crosses) and discrete data measured on a IWA-EP35 analyzer (red crosses) and linear regression relationships for the different data sets.

Title Page

Abstract

Introduction

Conclusions

References

Tables

Figures

◀

▶

◀

▶

Back

Close

Full Screen / Esc

Printer-friendly Version

Interactive Discussion



High-resolution continuous flow analysis setup for water isotopic measurement

B. D. Emanuelsson et al.

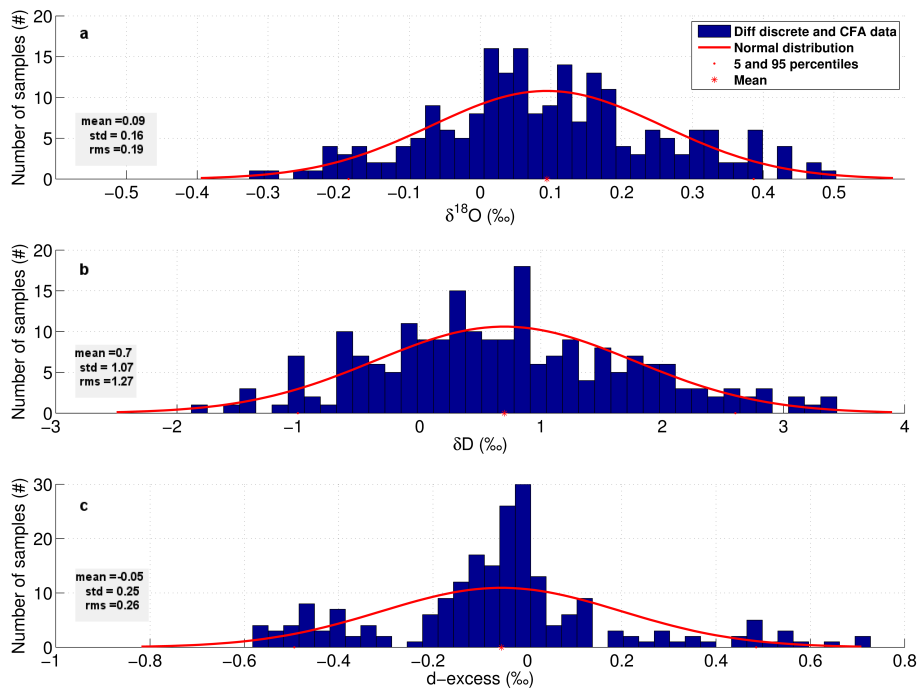


Figure 12. Histogram showing the difference between discrete and the CFA data; **(a)** for $\delta^{18}\text{O}$ **(b)** for δD and **(c)** d-excess for depths from 133 to 144 m of the RICE ice core.